



OTC 27414

Numerical Simulations of Ice Loads on Fixed and Floating Offshore Structures using the Discrete Element Method

Jiancheng (Jessie) Liu, Xiang Liu, Yingying Chen / American Bureau of Shipping;

Xue Long, Shunying Ji / Dalian University of Technology

Copyright 2016, Offshore Technology Conference

This paper was prepared for presentation at the Arctic Technology Conference held in St. John's, Newfoundland and Labrador, 24-26 October 2016.

This paper was selected for presentation by an ATC program committee following review of information contained in an abstract submitted by the author(s). Contents of the paper have not been reviewed by the Offshore Technology Conference and are subject to correction by the author(s). The material does not necessarily reflect any position of the Offshore Technology Conference, its officers, or members. Electronic reproduction, distribution, or storage of any part of this paper without the written consent of the Offshore Technology Conference is prohibited. Permission to reproduce in print is restricted to an abstract of not more than 300 words; illustrations may not be copied. The abstract must contain conspicuous acknowledgment of OTC copyright.

Abstract

Existing standards and codes do not comprehensively address and provide all necessary guidance and requirements for the design of Arctic offshore structures. Reliably assessing ice loads on offshore structures remains a challenge for industry, especially as “new” Arctic platform concepts are proposed for deployment in lighter ice operations, e.g. Arctic SEDU (Self-Elevating Drilling Units) and Arctic CSDU (Column-Stabilized Drilling Units). As a pragmatic solution, a comprehensive approach including relevant field measurements, physical model tests and numerical simulations is usually adopted in assessing the ice loads for a particular design. Field measurement results are limited in number and there is often uncertainty concerning actual ice conditions and load measurement techniques. Furthermore several data sets are constrained with proprietary restrictions. In particular no direct field data is available for the example “new” structures (SEDUs and CSDUs). Physical model tests always present challenges due to scale issues, ice property calibration, measurement uncertainties and high costs. Therefore, numerical simulations using the validated DEM tool based on the related field/model test data are anticipated to provide supplementary information for standards/rule-based designs.

ABS has expended efforts to develop practical and advanced tools to assess the ice loads on offshore structures for several years. One promising numerical approach, a graphic processing unit (GPU) based Discrete Element Method (DEM) model, processes the computations in parallel and solves the DEM model with millions of particles for complicated ice-structure interaction problems, e.g. ice simultaneously loading on multiple legs and ice loading on a large CSDU. The paper presents details of the developing ABS GPU-DEM tool, status of the verification program, plans for the current and the future developments and applications. Included are brief descriptions of background technologies, an approach to derive the DEM model bonding strength inputs, and validation studies of ice breakage simulations based on the Bohai Bay Jacket ice data. The ice load simulations for fixed and floating structures, i.e. jack-up legs and the Kulluk floating drilling platform, are also shown to demonstrate the tool’s capability and feasibility for Arctic offshore structure design. The interactions of ice and fixed/floating structures were analyzed, which provides useful references for future ice load modelling and offshore structure design.

1 Introduction

Oil-gas exploration in the Arctic is being hindered by the plunging price of oil, but drilling activities are anticipated to resume if market conditions recover. The following regions have suspended most exploration activity but there are possibilities to drill again in the future, Kara Sea; Chukchi Sea; Barents Sea & Norwegian Sea and Offshore Newfoundland and Labrador. Different drilling units are used at the different water depths. The shallow waters of the Kara and Chukchi Seas are well suited for jack-ups due to their highly efficient drilling capacity and mobility. Floating drilling units, e.g. semi-submersibles, are more appropriate for the deeper waters of the Barents Sea and Offshore Newfoundland and Labrador.

However, existing standards and codes don't provide all the necessary requirements and guidance for estimating ice loads for these types of Arctic structure designs, e.g. Arctic SEDU (Self-Elevating Drilling Unit) and Arctic CSDU (Column-Stabilized Drilling Units). Full-scale measurements are not available for these types of designs and physical model tests have difficulties in maintaining scale laws in addition to the measurement uncertainties and high costs. Therefore the numerical approach is expected to provide supplementary information in the standard/rule based designs.

As one promising numerical approach, ABS has partnered with Clarkson University (CU) and Dalian University of Technology (DUT) to develop a GPU-DEM model and its applications for numerically simulating various marine and offshore structures in ice since 2010. The GPU-DEM tool was initially designed for, but not limited to, modeling Arctic Self-Elevated Drilling Units (SEDU) in ice conditions. The work initially focused on numerical simulation of ice loads and global motion responses of fixed structures subject to various ice features including level ice, pack ice and first year ice ridges. Testing and validation efforts were led by ABS. Recent developments have been focused on simulation of ice loads on floating structures and incorporating six degree-of-freedom (DOF) motion and a nonlinear mooring system models considering multiple mooring lines.

This paper introduces the technical backgrounds of the developing GPU-based DEM tool including parallel computations, modeling ice sheets, and ice strength inputs for DEM model. The simulated ice breakages for level ice on the Bohai Jacket conical legs are compared with the field measurements as one validation of the tool's accuracy. In order to present the tool's capability and potential applications, scenarios of level ice loading on jack-up legs and the Kulluk floating drilling platform were simulated including a study on structure shape effects, load comparisons between shielded legs and truss legs, ice loads on a multi-legged structure, and interaction of ice and the floating structure. The simulations results were analyzed together with other publications, which offer useful references for future ice load modelling and offshore structure design.

2 Overview of DEM Tool

2.1 GPU-Based DEM Model

Due to limitations of the computational capacity of a typical CPU, traditional serial-computation technology cannot be extended to large scales. The CPU implementation of DEM can only support simple ice-structure interactions with less than the 50k particles, i.e. the simulation of level ice loading on one jacket leg. ABS has collaborated with DUT to develop a GPU-based DEM implementation that adopts parallel computation technologies and can be utilized to model a much larger number of discrete elements, thus providing a highly efficient approach for simulating the complicated interactions between the ice and the offshore structures (Di et al. 2014). The current GPU-based DEM tool supports modeling of over one million particles on a desktop computer with the NVIDIA Tesla K40 GPU card.

In order to verify the computational efficiency of GPU-DEM model against the CPU-DEM model, the scenario of balls falling down from a funnel container, as shown in Figure 1, was simulated using both implementations (Chang et al., 2012). In this comparison, the CPU was Intel Core i7 990X and the GPU was NVIDIA Tesla C205. The GPU running environment was Microsoft Visual Studio 2010 and CUDA 4.0. The compiler was NVCC4.0.

Table 1 presents the computational efficiency comparison results. When the particle number reaches 50k, the GPU computation time is only 1/36 of CPU's. The CPU cannot calculate the DEM model with more than 100k due to the serial system stack overflow.

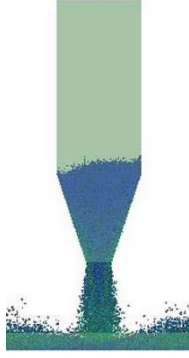


Figure 1 Snapshot of Particle Falling Simulation by DEM (Chang et al., 2012)

Table 1 Comparison of the computation time

Particles	GPU time (s)	CPU time (s)	CPU/GPU
1,000	132	1498	11.4
5,000	268	4663	17.4
10,000	318	8465	26.7
50,000	1017	36613	36.1
100,000	2354	-	-
1,000,000	355397	-	-

Note: '-' means the DEM model scale exceeds the CPU's capability due to serial system stack overflow.

2.2 Ice Strength Modelling

Bonded spherical particles are used to model the unbroken ice sheet in the DEM model as shown in Figure 2. The contacted spherical particles are bonded together using a parallel bond model, as the bonding disk in the figure. The maximum tensile and shear stresses acting on the bonding disk are calculated based on the beam theory as

$$\sigma_n = \frac{-|F_n|}{A} + \frac{|M_n|}{I} R \quad (1)$$

$$\tau = \frac{|F_s|}{A} + \frac{|M_s|}{J} R \quad (2)$$

Where, F_n is the force and M_n the moment in the normal direction. F_s is the force and M_s the moment in the shear direction. R is the particle diameter. The variables of A , I and J are defined as

$$A = \pi R^2 \quad (3)$$

$$J = \frac{1}{2} \pi R^4 \quad (4)$$

$$I = \frac{1}{4} \pi R^4 \quad (5)$$

If tensile stress or shear stress between two particles exceed the defined bonding strengths, then two particles de-bond. Using the above approach, different ice failure modes can be simulated in the DEM model including splitting, fracture, and flexure.

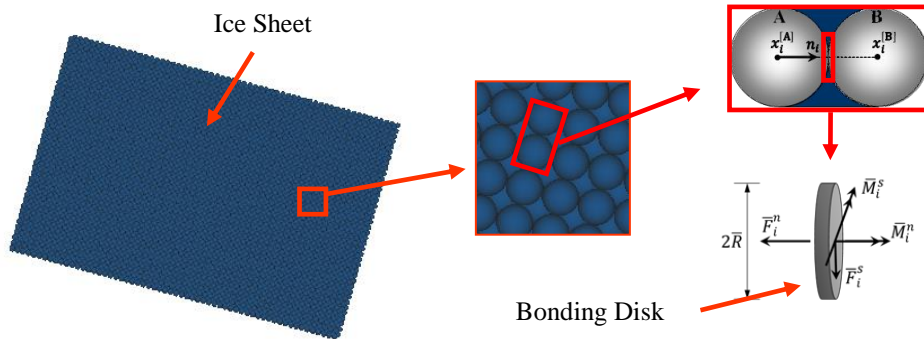


Figure 2. Modeling the ice sheet using spherical bonded elements in the DEM tool

In order to calibrate the relationship between the bonding strength parameters assumed in the DEM model and realistic ice strength terms, general ice sample tests of uniaxial compression test and 3-point bending test were simulated using DEM tool as shown in Figure 3.

It was found that the relative size of the particles to the simulated ice sample affect the simulated ice strengths even for the same bonding strengths. In order to simplify the problem, the shear bonding strength and normal bonding strength are kept the same in the test simulations. The below two equations were derived to set up the relationship between the bonding strength and ice strengths considering particle's relative size effects.

$$\sigma_c/\sigma_b = 6.85e^{-\bar{D}/0.4} - 0.35 \quad (6)$$

$$\sigma_f/\sigma_b = 2.78e^{-\bar{D}/0.2} + 0.38 \quad (7)$$

Where σ_c is the ice uniaxial compression strength, σ_f is the ice flexural strength, σ_b is the bonding strength, and \bar{D} is the relative particle size, which is equal to the reciprocal of the particle layer number of DEM model.

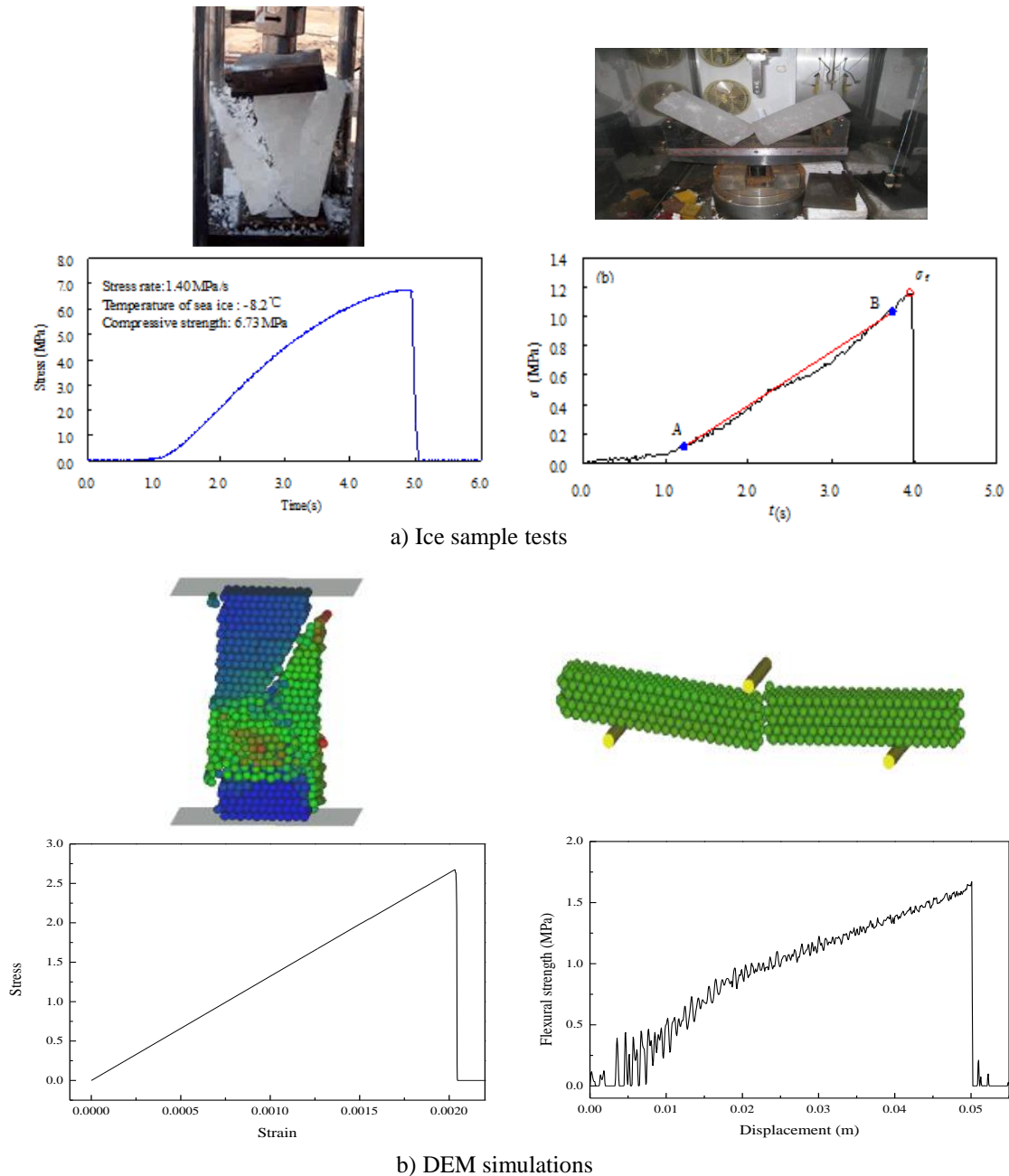
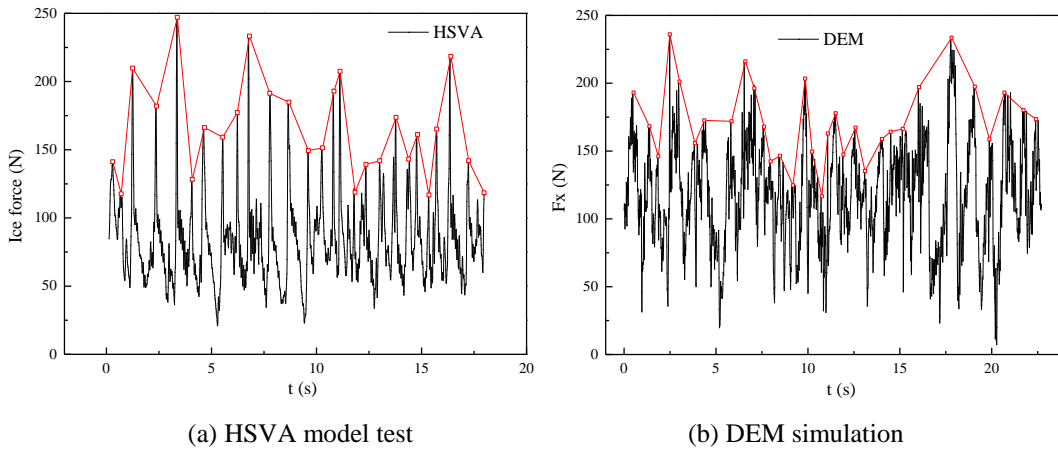


Figure 3. Ice sample tests and DEM simulations

More details on the DEM model theories and the bonding strength determinations can be referred to Ji et al., (2012) and Long et al. (2016)

3 Simulation of Ice Breakage Size

The DEM tool was validated against data collected on a Bohai Bay jacket structure and HVSA model test data for both cylindrical and conical waterline shapes. In the validation, the ice failure pattern, force time histories, ice load peak values and frequencies are compared with the field measurements. The detailed results were provided in publications by Ji et al. (2015, 2016). Figure 4 presents one example comparison between the HVSA model tests and DEM simulations.



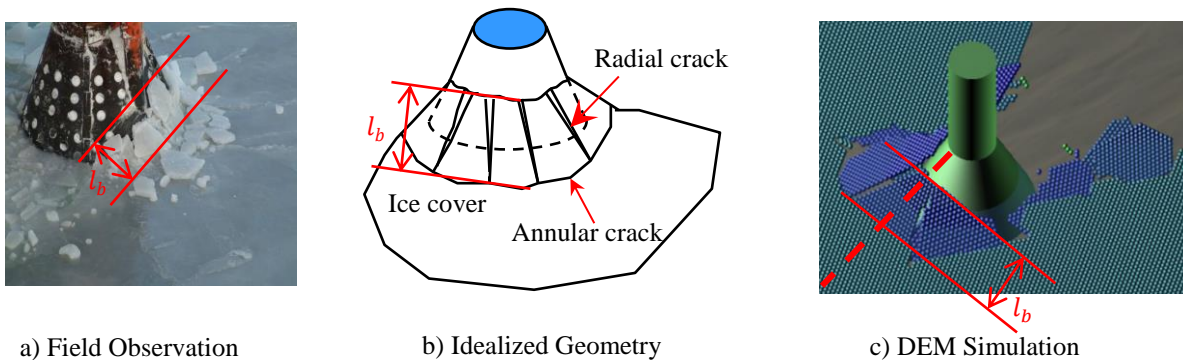
(a) HSVA model test (b) DEM simulation
 Fig 4 Comparison of model test and DEM simulation on ice loads on narrow conical structure (Long et al., 2016)

This section presents the validation of ice breakage parameters based on simulations of a level ice sheet broken by a conical leg and the Bohai Bay jacket structure field measurements. The bending failure of level ice manifests as two kinds of cracks: annular cracks and radial cracks as shown in Figures 4(a) and 4(b). The breakage length (l_b) is the radial distance of broken ice, which also determines the period of ice load in the process of bending failure. In the DEM simulations, the breakage length (l_b) is obtained by the maximum length of broken ice which happens to act on the front of conical structure as seen in Figure 5 (c).

The above DEM model simulations reproduced the field observations with decent agreement (Xu et al., 2011; Qu et al., 2006). The conical diameter at the water line affects the breakage length and flexural failure process. For small conical diameters, wedge-shaped failure modes (Figure 6(a)) occur first as radial cracks followed by annular cracks which appear once the broken ice length becomes large. For larger conical diameters, flexural failure initiates as annual cracks (Figure 6(b)) followed by relatively shorter radial cracks. This tends to create more plate-shaped pieces as opposed to wedge-shaped pieces of broken ice.

There is nearly a linear relationship between breakage length, l_b and ice thickness, h_{ice} . The ratio, l_b/h_{ice} typically stays within a certain range. In the field measurement data collected from structures in the Bohai Bay (Qu et al., 2006, Xu et al. 2011) , the ratios, l_b/h_{ice} , approximately follow up normal distribution as shown in Figure 7(a). It is noted the original Bohai Bay measured ice breakage size data is presented as the appearance frequencies of different ice breakage lengths, which is converted into the appearance probabilities of different ice breakage lengths in this paper. The DEM simulation results, shown in Figure 7(b), present a fairly good agreement with the field data in the distribution shape of the ratios of the breakage length and ice thickness. The ratios concentrate between 4 and 8.

The ice breaking length is affected by many factors as discussed by Lau et al. (1999). More studies are still needed to predict the ice breakages with high accuracy using the numerical approaches.



a) Field Observation (b) Idealized Geometry (c) DEM Simulation
 Figure 5 Breakage length of ice sheet in bending failure

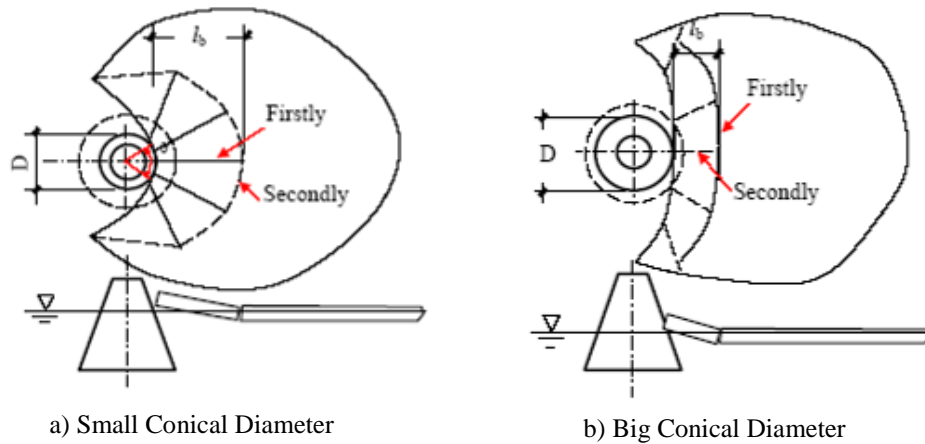


Figure 6 Conical diameter effects to ice breakage length

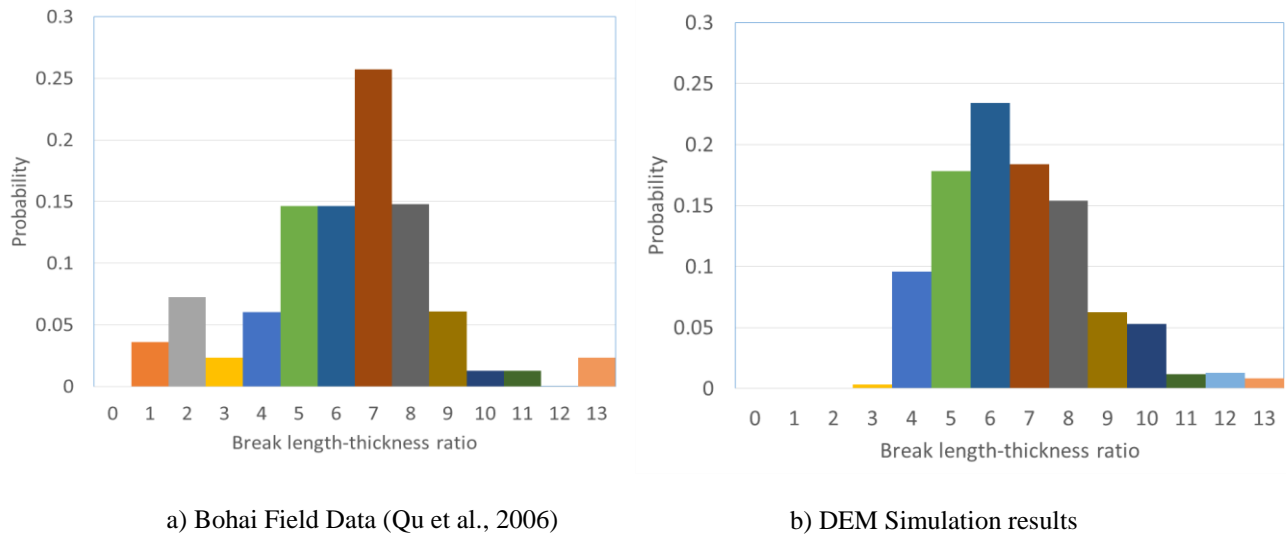


Figure 7 Probability distributions of ratio of ice breakage length to ice thickness

4 Simulation of Fixed Structure in Level Ice

The DEM tool is also utilized to model level ice interaction scenarios on vertically walled fixed structures. The fixed structures are modeled with 3 freedom dimensions, two horizontal displacements and one rotation in the vertical direction.

4.1 Structure Shape Effects

ISO 19906 (ISO, 2010) Section A.8.2.4.3.3 provides the following formula for global ice pressure on a vertical surface:

$$P_G = C_R \left(\frac{h}{h_1} \right)^n \left(\frac{w}{h} \right)^m \quad (8)$$

where w is the projected width of the structure, expressed in meters; h is the thickness of the ice sheet, expressed in meters; h_1 is a reference thickness of 1 m; m is an empirical coefficient equal to -0.16 ; n is an empirical coefficient, equal to $-0.50 + h/5$ for $h < 1.0$ m, and to -0.30 for $h \geq 1.0$ m; C_R is the ice strength coefficient, expressed in MPa.

The formula does not take into account the effects of the structural shape but experience suggests that a wedge shaped structure penetrating an ice sheet faces less resistance than a flat structure at the same width. In an effort to explore the structural shape effects, DEM was used to simulate a level ice sheet interacting with three different leg geometries shown in Figure 8. In the figure, the black shape represents a broadside ice drift direction against a square-shaped leg, the red shape is the diagonal direction, and the purple structure is a round leg shape. The edge length of the square leg is 10 m (Liu, 2013).

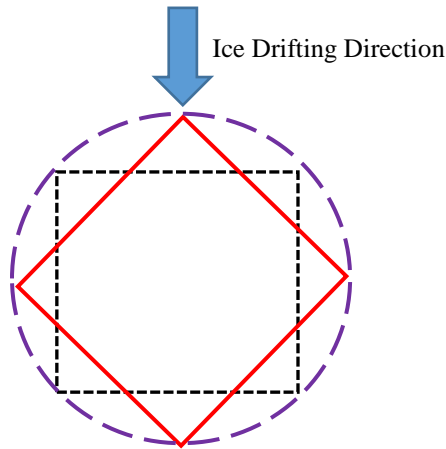


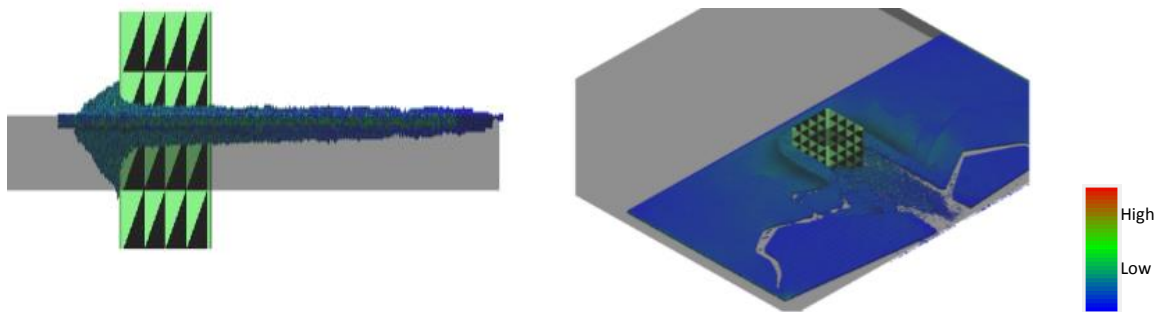
Figure 8 Schematic diagrams of three type of legs loaded by ice.

The area of the modeled ice sheet needs to be large enough to eliminate effects of the boundary conditions on the ice loading process. The ice is pushed towards the structure at the constant velocity, 1.0 m/s. According to equation (6), the bonding strength, 0.428 MPa, corresponds to an ice uniaxial compression strength of 1.62 MPa. The parameters of the DEM model for the ice sheet moving through the legs are provided in the Table 2.

Table 2 Parameters of DEM model for level ice-leg interactions

Definition	Symbol	Values
Sea ice Density	ρ	920 kg/m ³
Ice thickness	t_i	1m
Particle layer number	N_p	5
Shear bonding strength	σ_b^s	0.428 MPa
Normal bonding strength	σ_b^n	0.428 MPa
Particle-particle friction	μ_{pp}	0.1
Structure-particle friction	μ_{wp}	0.03
Drag coefficient of fluid	C_d	0.05
Leg equivalent mass	M_{pile}	1000 ton
Leg Spring Stiffness	K_{pile}	7.5×10^3 kN/m
Leg damping ratio	ζ_{pile}	0.07
Rotational Spring Stiffness		Fixed

Figure 9 presents snapshots of the DEM simulations of a level ice sheet moving through each of the three leg geometries. The colors of the particles represent the internal forces between particles.



a) Broadside direction

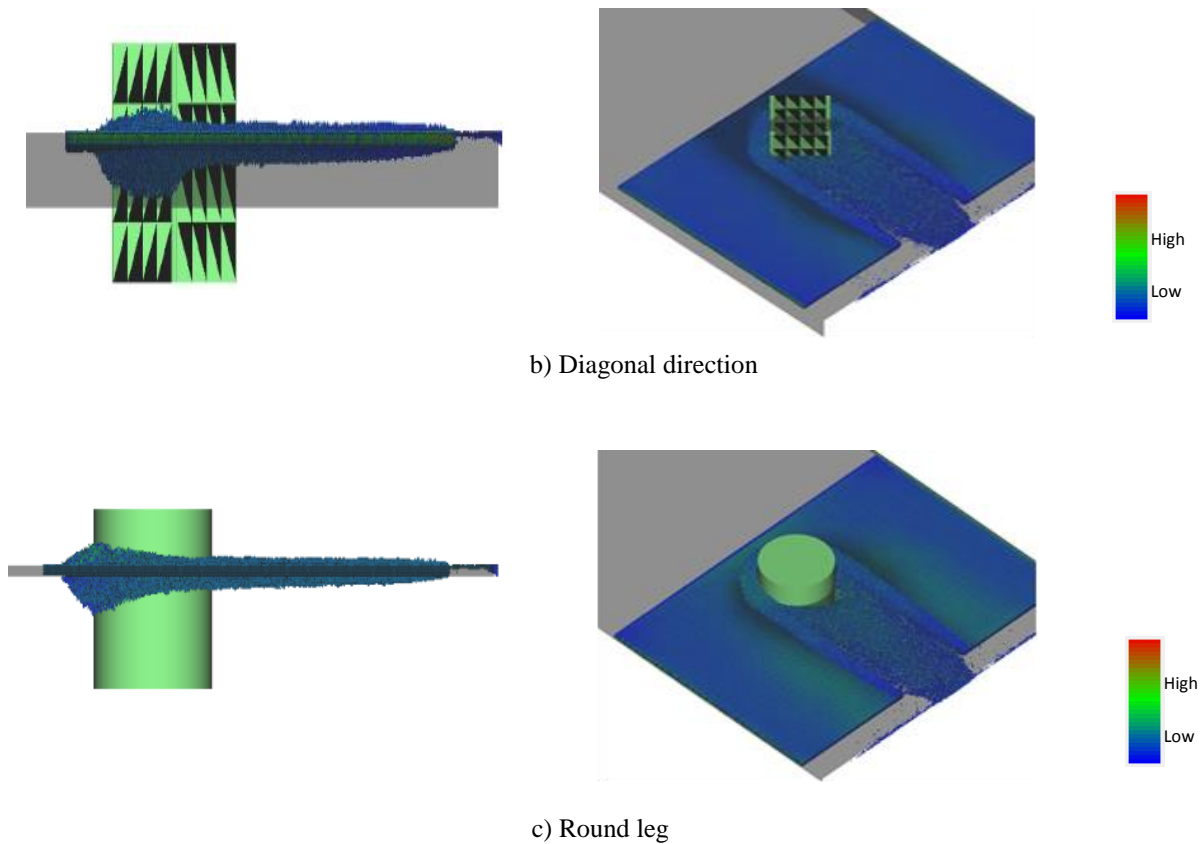


Figure 9 Snapshots of DEM simulations of an ice sheet moving through legs

The following behavior was observed:

- The particles around the leg are de-bonded due to the leg's penetration into the ice sheet. The de-bonded particles, which represent crushed and broken ice pieces, pile up in front and around the sides of the legs. As the ice clears around the structure, a channel forms with broken ice pieces forming its edges
- The internal forces are relatively high around the leg compared with low internal forces far away from the leg. This verifies the boundaries of the ice sheet model has a fairly small effect on the ice-leg interactions.
- A larger area of high internal forces and more broken ice pieces piling up in front of the broadside case suggests that the ice breaking and ice clearing process is more difficult on a flat vertical surface than for the rounded and wedge-shaped interface geometries.

Figures, 10 to 12, present the calculated force-time histories using the DEM tool. Fluctuating forces are observed in all three scenarios with fairly steady peak force frequencies and magnitudes. In the figures, the red curves represent the peak force values.

Per ISO 19906 Section, A.8.2.4.3.4, the strength index (here it is the compression strength), 2.07 MPa, is for the area where the strength parameter, $C_R=1.8$ MPa. In the simulation, the ice compression strength is 1.63 MPa, which corresponds the strength parameter, $C_R=1.4$ MPa. Using the ISO 19906 formula A.8-19 and A.8-21, the global ice loads on the legs can be estimated and the results are listed in Table 3.

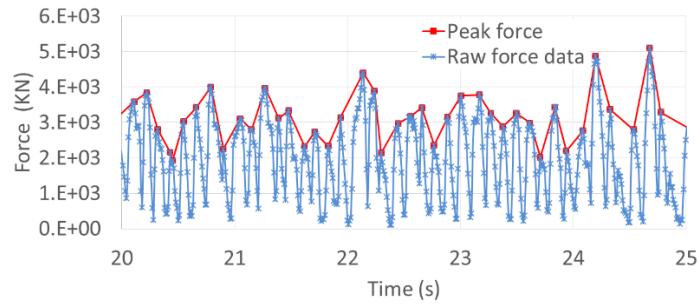


Figure 10 Ice force time history and peak selections when ice moving at broadside direction

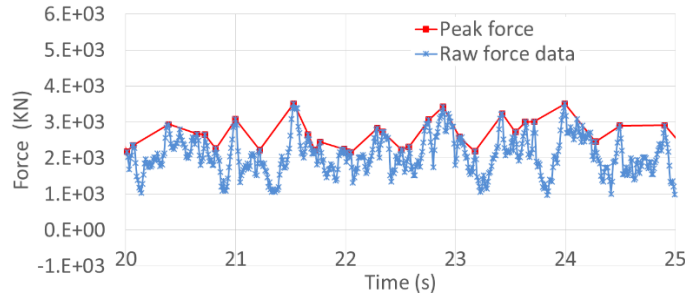


Figure 11 Ice force time history and peak selections when ice moving at diagonal direction

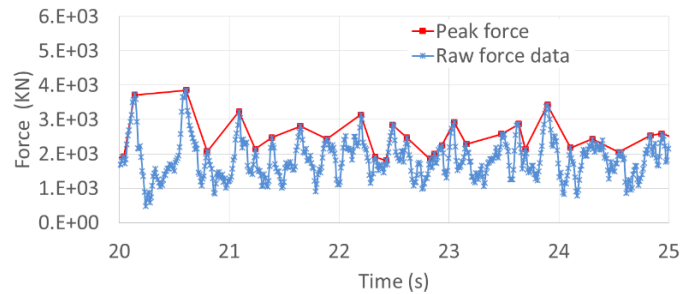


Figure 22 Ice force time history and peak selections when ice moving through round leg

Table 3 Ice forces from DEM simulations and ISO 19906

	Unit	Broadside	Diagonal	Round
Average peak force (Fmean)	MN	3.2	2.6	2.4
Exceedance probability = 0.01 (Pe=0.01)	MN	5.0	3.5	3.5
Maximum peak force (Fmax)	MN	6.8	3.8	3.9
ISO 19906 formula value (FISO)	MN	11.8	15.9	15.9
Fmax/FISO		57%	24%	24%

A few observations are obtained from this study of structural shape effects:

- a. The simulated ice force is less than 60% of the ISO 19906 formula value for the broadside direction case.
- b. The average and maximum peak ice forces simulated by DEM are both larger for the broadside case compared with the diagonal and round geometries but ISO 19906, which is based on projected area, suggests otherwise.

As another way to compare the shape effects, consider the shape factor for the flat surface structure is 1.0 and the shape factors of the other geometries is determined by the ratio of the ice force on the considered structure to the ice force on the flat surface structure for same projected loading area (width and height). Figure 13 presents this comparison based on the DEM simulation results. The geometrical effects considered by other offshore structures standards - SNIp, VSN, API RP 2N and Q/HSn - as well as simulation results from the Particle-ice-Cell (PIC) method, another numerical modeling approach (Sayed, et al. 2000), are listed in Table 4.

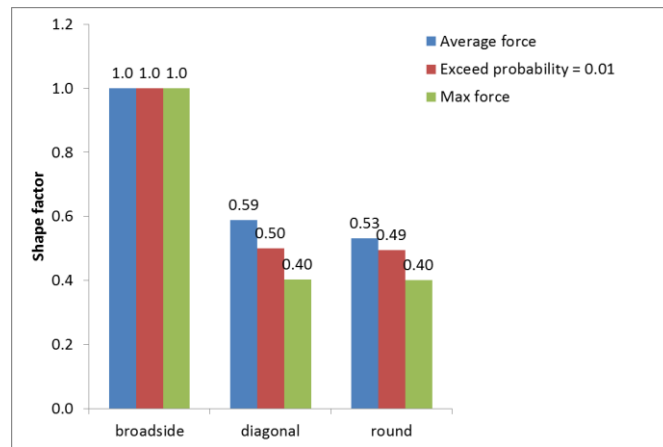


Figure 13 Acquired shape factors based on DEM model simulation results

Table 4. Comparison of the shape factors for the diagonal case

Reference	Shape factor	Notes
SNIP (1995)	0.58	Upper bound
VSN (1998)	0.9	multi-face
API RP 2N (1995)	0.73	Wedge case
CNOOC code (Q/Hsn)	0.7	Diam. < 2.5 m
PIC (Sayed, et al., 2000)	0.7	Peak max
DEM	0.6	Peak max

It can be observed that the shape factors obtained in the DEM simulations range between 0.53 and 0.59, which are lower than the values prescribed by existing standard/codes, 0.58~0.9, but the discrepancy is not significant. The results from another numerical simulations approach (PIC) shows reasonable agreement with DEM.

4.2 Shielded Leg and Truss Leg

Different types of jack-up leg structures (truss and shielded legs) have been proposed for operations in ice conditions but existing codes do not adequately provide design ice load criteria for these arrangements (Di, S., et al., 2014). DEM was used as a method to model the ice loading process on both truss and shielded-type jack-up leg arrangements. The same ice sheet and model parameters listed in Table 2 were used in this analysis. The chord distances of both leg arrangements were kept the same.

Figure 14 presents a snapshot of a simulated level ice sheet moving through the truss-type leg arrangement. The ice sheet is initially broken by the forward-most leg members. Some broken pieces flow into the leg, and then are further broken into smaller ice pieces by the additional leg members before they move out the leg, as shown in Figure 14.

Some ice pieces remain inside the leg, as shown in Figure 14. One concern about the use of truss-type jack-up legs in ice conditions is the refreezing of broken ice and brash ice inside the leg structures. If broken ice pieces become trapped and can't clear out quickly, they may become refrozen and result in an ice jamming situation within leg.

Compared to the shielded-type leg, as shown in [错误!未找到引用源。 9-a\)](#), high internal forces between particles distribute within a smaller area as the ice sheet breaks against the open truss structures. As a result, DEM predicts lower ice forces for the truss-type leg.

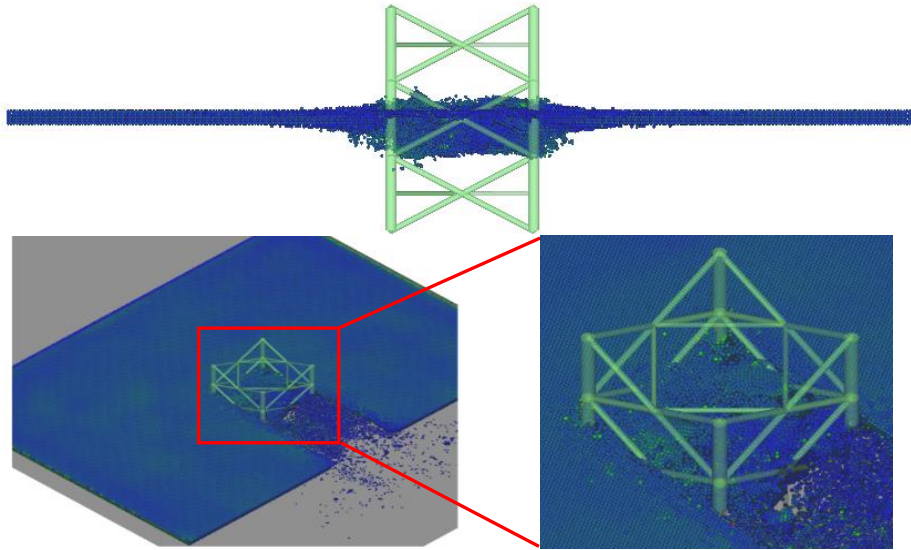


Figure 14 Snapshot of the simulated ice sheet moving through truss leg

Table 5 presents a comparison of peak ice force for the truss and shielded-type jack-up leg arrangements. DEM predicts the global ice load on the truss-type leg is much smaller than the shielded leg, about 30% for this case. It is noted that the relatively smaller global ice load doesn't necessarily suggest the truss design is better suited for ice conditions. One must evaluate the structural capacity of each design including the chords, shield, and truss structures subject to the local ice load distributions. The DEM tool allows users to model realistic interactions and extract the appropriate forces and pressures for such an analysis.

Table 5. Comparison of the peak forces on trussed leg and shielded leg.

	Unit	Truss	Shield	Truss/Shield
Average peak force (F_mean)	kN	969	3163	0.31
Exceedance probability=0.01 (Pe=0.01)	kN	1679	5015	0.33
Maximum peak force (F_max)	kN	2144	6795	0.32

4.3 Ice Loads on Multiple Legs

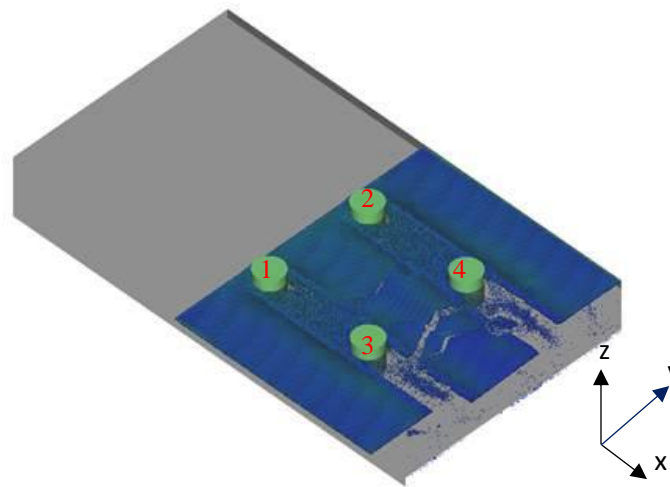
In this section, the DEM tool is used to simulate a level ice sheet moving through four round legs. The structure has two translational degrees of freedom in the horizontal plane and one rotational degree of freedom around the vertical axis. The assumed structural parameters are listed in Table 6. The same round leg geometry presented in Figure 8 is used here and the distance between each leg is 55 m. The same ice sheet and model parameters listed in Table 2 are used.

Table 6 Parameters of Structural Model

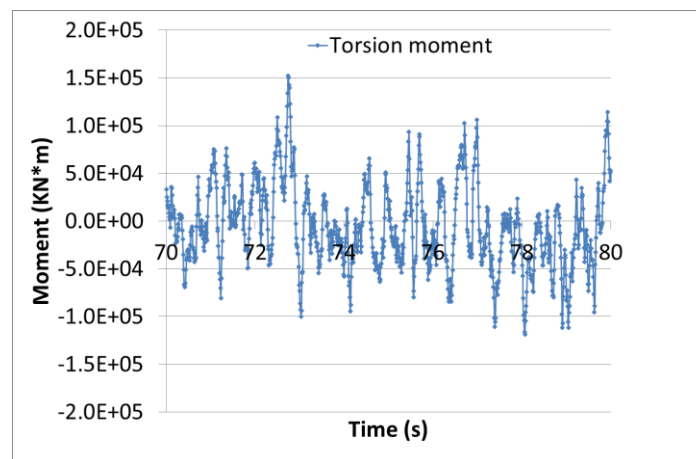
Definition	Symbol	Values
Structure mass	$M_{structure}$	80 kton
Spring Stiffness	$K_{structure}$	8.0×10^3 kN/m
Damping ratio	$\zeta_{structure}$	0.07
Moment of Inertia	$I_{torsion}$	$3.91e10$ kg*m ²
Torsional spring stiffness	$K_{torsion}$	$1.35e9$ N*m
Torsional damp ratio	$\zeta_{torsion}$	0.07

Figure 15 presents a snapshot of simulation results and calculated ice force time histories for the multi-legged structure. Torsional moments are observed from the simulation results, which is caused by a force imbalance between the four legs due to non-simultaneous ice failure during the interaction. The torsional moment frequency appears similar to the force frequencies on each leg as shown in Figure 15 b), c) and d). These DEM simulation results suggest that torsional moments from ice actions should be considered in the design of multi-legged Arctic offshore structures.

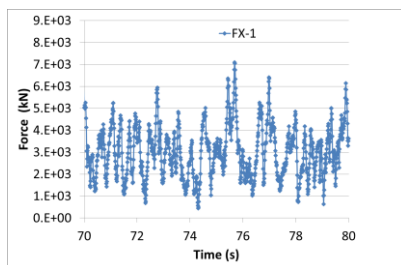
The highest ice force values are observed on the forward legs in the x-direction (FX-1, aligned with ice drift direction). The peak ice force in the y-direction (FY-1, perpendicular to ice drift) is about half of the value in the x-direction. The rear legs experience very small ice forces in this scenario since the load is sheltered by the forward legs.



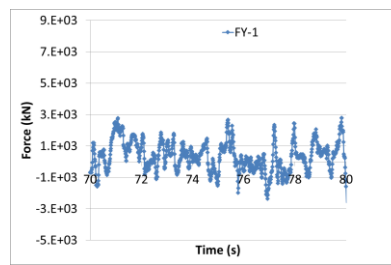
(a)



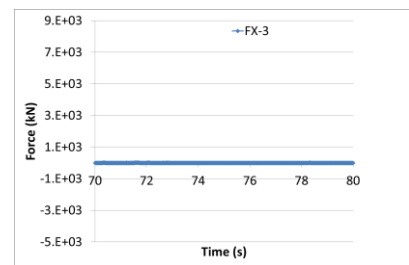
(b)



(c)



(d)



(e)

Figure 15 Snapshot of DEM simulation results and calculated ice forces.

5 Simulation of Floating Structures in Level Ice

Ice loads on floating structures in ice conditions is a recognized challenge that several researchers have approached using numerical methods. (Kubat et al., 2011; Sayed, et al., 2015; Daley, et al., 2014; Metrikin, et al., 2015) Recent developments of the DEM tool have focused on the modeling of moored floating structures in ice. The structure is modeled as a rigid body with 6 degrees of freedoms. Current forces, buoyancy forces, mooring forces and Dynamic Positioning (DP) thruster forces are all considered, along with the ice forces, when calculating the floating structure motions and responses.

5.1 Mooring Model

The restoring force from the mooring system due to global motions of the floating structure is modeled in the DEM simulation. Damping effects are neglected considering they have little influence on the quasi-static global ice load assessments. A linear spring model for floating body analysis has been found in some previous studies to be a suitable approximation (Hong et al., 2005; Tang et al., 2011), and therefore is applied in the DEM simulation. As shown in Figure 16, one end of the mooring line is fixed at the sea bottom, Point A, while the other is connected to the structure, Point B. The X' axis is the projected line of the mooring line, from point A to point B, at the horizontal plane.

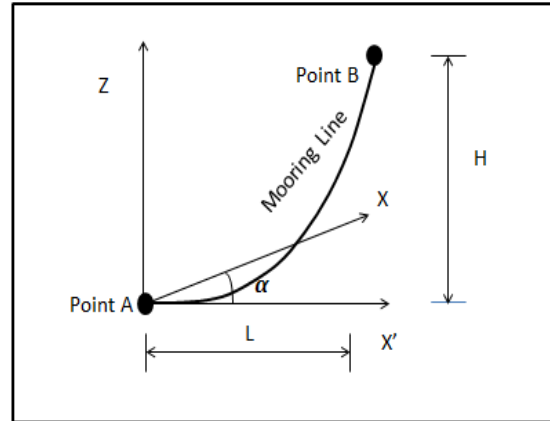


Figure 16 Schematic of a mooring line

The internal forces in the mooring line can be written as:

$$T = k \cdot \Delta L \quad (9)$$

Where, k is the parameter of the linear mooring line and ΔL is the horizontal offset of the moored point. The details can be found in the references by Hong et al. (2005) and Tang et al. (2011).

5.2 Simulation of Kulluk in level ice

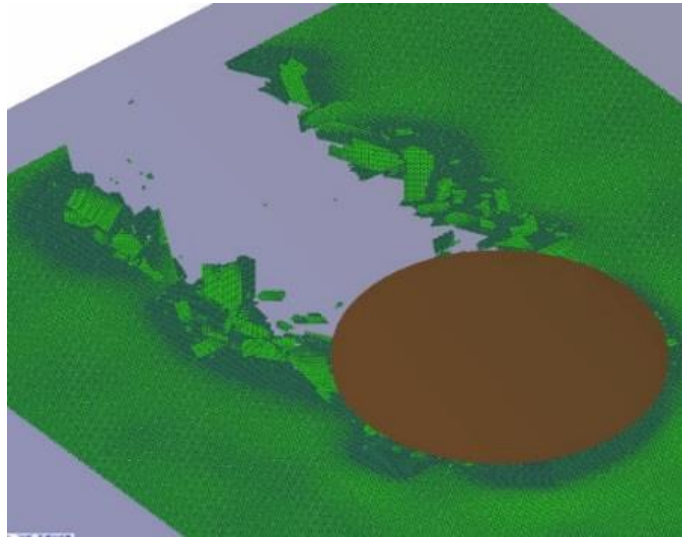
The Kulluk drilling barge was a floating Arctic offshore structure deployed in the 1980s during Canadian and US Arctic offshore exploration campaigns. The Kulluk had a downward sloping circular hull form designed to break ice in flexure at relatively low force levels. Below the waterline there was an outward flare, to ensure that broken ice pieces cleared around the structure and did not enter the moon pool or become entangled in the mooring lines, (Wright, 2000).

DEM is used to simulate the Kulluk platform operating in nominal level ice conditions. Table 7 lists the parameters assumed in the DEM model.

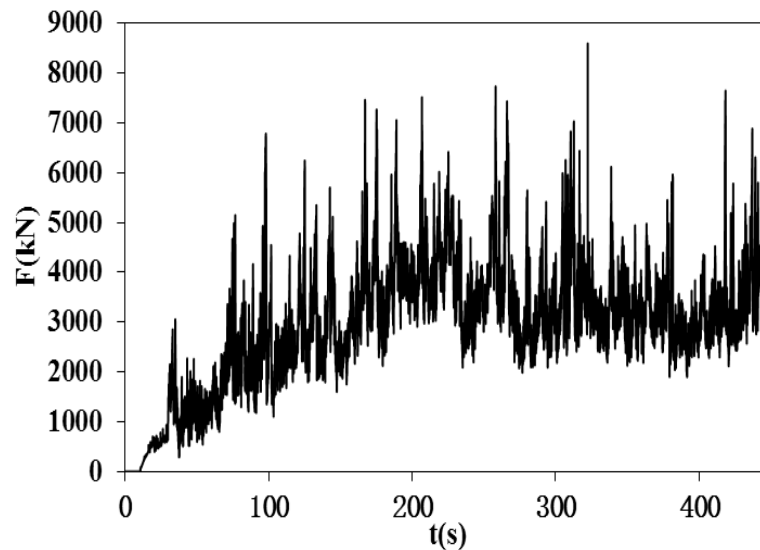
Table 7 Parameters of DEM model for level ice-Kulluk interactions

Definition	Symbol	Value
Water depth		200 m
Ice thickness	h	0.75 m
Particle layer number	-	1
Friction coefficient	μ	0.2
Bond strength of normal	σ_b^n	0.5MPa
Bond strength of tangential	σ_b^s	0.5MPa
Velocity of ice	v_p	0.5 m/s
Number of mooring lines	N	4
Length of mooring lines	L	734.9m
Unit weight of mooring line	w	3361N/m
Stiffness of mooring line	k	1.0 MN/m
Kulluk deck diameter	D_{deck}	81 m
Kulluk water line diameter	D	70 m
Draft	T	11.5m

Definition	Symbol	Value
Displacement	Dis	2800 ton
Length of mooring lines	L	734.85m
Unit weight of mooring line	w	3361N/m



(a)



(b)

Figure 17 Snapshot of the simulated ice sheet moving through Kulluk and global ice loads

Figure 17 a) shows that the hull form provides the unit with good icebreaking and ice clearance capabilities. The level ice is primarily broken due to the flexural failure type. Figure 17 b) shows the total ice force time history on Kulluk. The initial encounter between the ice and the Kulluk produces a peak force of just over 3.0 MN. Subsequent loading events show several peaks between 7-9 MN. The first force peak occurs when the initial macro ice crack is broken. The subsequent force peaks reflect the continuous level icebreaking which is affected by the ice edge shape and ice blocks left in the previous ice-structure interactions, and therefore more complicated.

Figure 18 presents the simulated Kulluk motion responses. The initial surge reaches 1.0 m and the following peak surge event reaches 2.98 m. The frequency of the Kulluk motion responses are much lower than the frequency of the ice forces, as shown in Figure 16 b). The behavior is governed by the natural frequency of the moored system. The stiffness of the mooring line

significantly affect the offset amplitude and frequency. Ongoing work is being carried out to consider longer simulations and includes analysis of peak force statistics and frequency/amplitude analyses of the motion response of Kulluk.

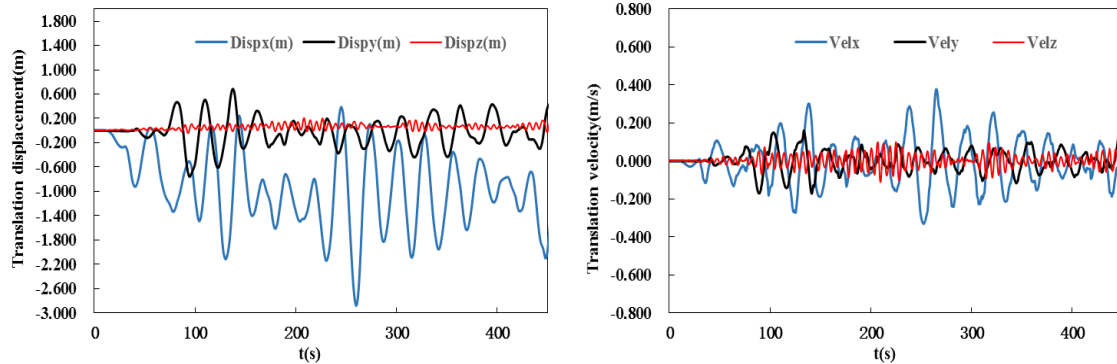


Figure 18 The Kulluk offset time histories in six degrees

The GPU-DEM tool has the functional capability to simulate moored floating structures in ice. The results presented here reflect the physical process of the ice-structure interactions and are reasonable based on engineering judgements. Further quantitative validations based on field/model test data, including the actual Kulluk field measurement dataset, is being carried out. The application to floating structures will be an important working focus in the continued development of the ABS GPU-DEM tool.

6 Summary and Recommendations

A GPU-based DEM tool to numerically predict level ice actions on the fixed/floating offshore structures is presented in this paper. The tool utilizes parallel computation technologies to solve large scale DEM model for simulating complicated ice-structure interaction scenarios. The modeled ice conditions by the DEM tool include level ice, pack ice and ice ridges. The modeling of the level ice conditions is presented and discussed in this paper. The validated tool is for ABS' clients to seek the supplementary information in rule/standard based offshore structure designs.

Different ice failure modes are modelled through the de-bonding of initially bonded discrete particles in the DEM model. The ice strength parameters are input as bonding strengths in the model and calibrated using uniaxial compression and 3-point bending ice sample tests. The tool has checked using validation case studies based on the Bohai Bay jacket structure data and model test data. Validation simulations of ice breakage size on conical shaped structures were presented in the paper. Level ice loads on the different leg geometries and multi-legged structure were simulated and discussed to explore structure shape effects, differences between truss-type and shielded jack-up legs, and ice loads on multi-legged structures. Finally the moored Kulluk in level ice was simulated to demonstrate the tool's capability and potential applications. The results provide the references for the future numerical modeling of ice-structure interactions and Arctic offshore structure designs.

Assessing ice-structure interactions is a complicated process in Arctic offshore structures designs and codes/standards offer the limited guidance. Numerical simulations are expected to provide some supplemental information. The DEM simulation results presented in this paper are promising, but the accuracy and reliability of the tool still requires more validation studies and developments. ABS and DUT are continuing a collaborative effort to develop a practical and robust tool that designers and engineers can use as a supplement to rule/standard-based offshore structure designs.

Acknowledgements

The authors would like to acknowledge ABS for allowing the publication of this paper. Throughout the work, valuable discussions and supports were received from James Bond, Han Yu, Jer-Fang Wu, Shewen Liu, Jie Xia and other ABS colleagues. All of them are acknowledged greatly.

Reference

- API, 1995, Recommended Practice for Planning, Designing, and Constructing Structures and Pipelines for Arctic Conditions, API RP 2N.
- Chang, X., Wang, Y., Di, S., He, G., Ji, S., 2012, GPU-Based Parallel Computaton for Particle Discrete Element, National Conference on Computational Mechanics of Granular Materials, Hunan, P.R.China.
- Daley, C., Peters, D., Blades, G., & Colbourne, B., 2014, Simulation of Managed Sea Ice Loads on a Floating Offshore Platform using GPU-Event Mechanics. International Conference and Exhibition on Performance of Ships and Structures in Ice, IceTech'14. Banff, AB, Canada.
- Di, S., Ji, S, Liu, J., Yu, H., 2014, Discrete Element Method Helps Determine Load Level for Ice-Capable Jackups, Arctic

- Technology Conference, Texas, USA, OTC Paper 1770869.
- Lau, M., Molgaard, J., Williams, M., Arisi, S., Swamidas, J., 1999. An analysis of ice breaking pattern and ice piece size around sloping structures. 18th International Conference on Offshore Mechanics and Arctic Engineering—OMAE99. St. John's, Newfoundland, Canada, pp. 199 - 207 (July 11 - 16).
- Long, X., Ji, S., 2016, Discrete Element Simulation of Sea Ice Loads on Narrow Conical Structures, The 23rd IAHR International Symposium on Ice. Ann Arbor, Michigan USA.
- Hong, S., Kim, J., Cho, S., et al. 2005, Numerical and Experimental Study on Hydrodynamic Interaction of Side-by-side Moored Multiple Vessels [J]. *Ocean Engineering*, 32(7):783–801.
- ISO, 2010, ISO 19906 Petroleum and Natural Gas Industries – Arctic Offshore Structures.
- Ji, S., Li, Z., Liu, S., 2012, Discrete Element Simulation of Sea Ice Flexural Strength, 21st IAHR International Symposium on Ice, Dalian, China.
- Ji, S., Di, S., Liu, S. 2015, Analysis of Ice Load on Conical Structure with Discrete Element Method, *Engineering Computations*, 32(4):1121-1134.
- Ji, S., Sun, S., Long, X., et al., 2016, Discrete Element Modeling of Ice Loads on Ship and Offshore Structures, The 7th International Conference on Discrete Element Methods, Dalian, China.
- Kubat, I., Wright, B., Iyerusalimskiy, A., et al, 2011, Numerical Simulations of Ice Interaction with a Moored Structure[C]. Arctic Technology Conference. Houston, Texas, USA
- Liu, J., 2013, Ice Load Assessment for Jack-Up Units, Proceedings of the 22nd International Conference on Port and Ocean Engineering under Arctic Conditions (POAC'13), Espoo, Finland.
- Metrikov, I., Gürtner, A., Bonnemaire, B., Tan, X., Fredriksen, A., & Sapelnikov, D. (2015). SIBIS : A Numerical Environment for Simulating Offshore Operations in Discontinuous Ice. *Port and Ocean Engineering under Arctic Conditions, POAC'15*. Trondheim, Norway.
- Q/Hsn 3000-2002, 2002, Regulations for Offshore Ice Condition & Application in China Sea, China National Offshore Oil Corporation Standard (CNOOC code)
- Qu, Y., Yue, Q., Bi, X., Kärnä T., 2006, A Random Ice Force Model for Narrow Conical Structures [J]. *Cold Regions Science and Technology*, 45:148 - 157.
- Sayed, M., Frederking R., Barker A., 2000, Numerical Simulation of Broken Ice Cover Forces on Structures: a Parametric Study, Proceedings of the 10th International Offshore and Polar Engineering Conference, ISOPE'00, Vol. 1, pp 656-662, Seattle, USA.
- Sayed, M., Kubat, I., Watson, D., Wright, B., Gash, R., & Millan, J. (2015). Simulations of the Station Keeping of Drillships under Changing Direction of Ice Movement (OTC 25565). Arctic Technology Conference, ATC'15 (pp. 1–15). Copenhagen, Denmark.
- SNiP, 1995, Loads and Effects on Hydrotechnical Facilities (Caused by Waves, Ice, Vessels), Construction Codes and Regulations, Moscow, SNiP 2.06.04-82
- Tang, H., Huang, C., Chen, W., 2011, Dynamics of Dual Pontoon Floating Structure for Cage Aquaculture in a Two-Dimensional Numerical Wave Tank [J]. *Journal of Fluids and Structures*, 27(7):918–936.
- Wright, B., 2000, Full Scale Experience with Kulluk Stationkeeping Operations in Pack Ice (PERD/CHC Report 25-44).
- VSN, 1988, Design of Ice-Resistant Stationary Platforms, Ministry of the Oil Industry of the USSR, Moscow, VSN 41.88.
- Xu, N., Yue, Q., Qu, Y., et al., 2011, Results of Field Monitoring on Ice Actions on Conical Structures, *Journal of Offshore Mechanics and Arctic Engineering*, 133: 041502-8.